Full Paper

ELECTROANALYSIS

Evaluation of Gibbs Energy of Dioxouranium Transfer at an Electrified Liquid|Liquid Interface Supported on a Microhole

Tom J. Stockmann,[a] *Astrid J. Olaya*,[b] *Manuel A. Méndez*,[b] *Hubert H. Girault*,[b] *Zhifeng Ding*[*a]

[a] Department of Chemistry, The University of Western Ontario, Chemistry Building, 1151 Richmond Street, London, Ontario, Canada N6A 5B7
  URL: http://publish.uwo.ca/~zfding/
[b] Laboratoire d'Electrochimie Physique et Analytique, Station 6, École Polytechnique Fédérale de Lausanne, Lausanne, Switzerland CH-1015
*e-mail: zfding@uwo.ca

Abstract
Herein is reported the determination of the Gibbs energy of dioxouranium (UO_2^{2+}) transfer across an interface between two immiscible electrolytic solutions (ITIES), water and 1,2-dichloroethane, that was supported at a 25 μm diameter microhole, by means of linear sweep voltammetry. Through the use of minimal to no supporting electrolyte, this technique is able to observe ion transfer (IT) of extremely hydrophilic ions voltammetrically. As the applied potential in the aqueous phase became increasingly positive the UO_2^{2+} ions were driven into the organic phase resulting in IT. The standard transfer potential, $\Delta_o^w\phi^{\circ\prime}$ was determined to be 0.865 V through a novel curve fitting methodology applied directly to the voltammogram. The Gibbs energy of transfer was calculated to be 167 kJ·mol^{-1}. Additionally, the kinetics of IT was explored using a Butler–Volmer model through finite element analysis, whereby the voltammetric current response owning to migration effects in the experimental CVs was approximated in the overlaid, simulated CVs using slow reaction kinetics.

Keywords: Butler–Volmer model, Gibbs energy of transfer, ITIES, Microhole, Uranyl or dioxouranium

1 Introduction

Dioxouranium or uranyl (UO_2^{2+}) is the most common oxidation and chemical state of uranium in nuclear waste recycling [1,2]. After removal from the nuclear fuel chamber the spent fuel pellets are dissolved into an aqueous solution via concentrated nitric acid [1,2] for the purpose of separating the uranium from its neutron absorbing fission byproducts via solvent extraction. The PUREX (Plutonium Uranium Extraction) process of solvent extraction, between water and a paraffinic organic solvent like *n*-dodecane, utilizes an organic ligand, or complexing agent, like tributylphosphate (TBP) [1,2] and has been described by the following chemical reaction of UO_2^{2+} with TBP:

$$UO_2^{2+}(aq) + 2NO^-_3(aq) + 2TBP(org) \rightarrow$$
$$UO_2(NO_3)_2TBP_2(org) \qquad (1)$$
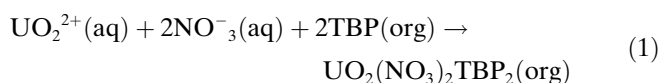
Of particular interest is the measurement and evaluation of the effectiveness of ligands towards metals species for the purpose of determining their selectivity. One possible avenue, whereby direct thermodynamic data concerning complexation reactions can be obtained is through the facile use of voltammetric techniques at the interface between two immiscible electrolytic solutions (ITIES) [3–6]. A typical ITIES is the interface between water and 1,2-dichloroethane (DCE) [3,4,7–13]. A potential can be applied across the interface where ions are transferred across the ITIES through a push/pull mechanism. This process can be generalized as follows [14,15]:

$$i_w^{zi} \underset{k_b}{\overset{k_f}{\rightleftharpoons}} i_o^{zi} \qquad (2)$$

where species i, with charge z_i, transfers from phase w (aqueous phase) to phase o (organic or DCE phase). This process is referred to as simple ion transfer (IT) and each ionic species has a unique standard transfer potential, $\Delta_o^w\phi^\circ$, analogous to the standard redox potential, E°, found in conventional electrochemistry, and is described, for a general case at the ITIES, w|o, by the following:

$$\Delta_\alpha^\beta\phi_i = \Delta_\alpha^\beta\phi_i^\circ + \frac{RT}{z_iF}\ln\left(\frac{a_\alpha^i}{a_\beta^i}\right) = \Delta_\alpha^\beta\phi_i^\circ + \frac{RT}{z_iF}\ln\left(\frac{\gamma_\alpha^i}{\gamma_\beta^i}\right) + \frac{RT}{z_iF}\ln\left(\frac{c_\alpha^i}{c_\beta^i}\right)$$
$$= \Delta_\alpha^\beta\phi_i^{\circ\prime} + \frac{RT}{z_iF}\ln\left(\frac{c_\alpha^i}{c_\beta^i}\right) \qquad (3)$$

where a_α^i, γ_α^i, and c_α^i are the activity, activity coefficient, and concentration of species i in phase α. The terms in phase β are similar to those in phase α. The formal transfer potential, $\Delta_o^w \phi^{\circ\prime}$, (shown on the right of Equation 3) is achieved if the concentrations of the charged species are used. Several comprehensive reviews on electrochemistry at the ITIES are available [14–17]. Analogous to conventional solvent metal extraction, ligands, L, can be used to facilitated ion transfer (FIT) processes through the following reaction:

$$i_w^{zi} + nL_0 \underset{k_b}{\overset{k_f}{\longleftrightarrow}} iL_{n,0}^{zi} \qquad (4)$$

Indeed, if i_w^{zi} and L are replaced with UO_2^{2+} and TBP respectively then this would be the electrochemical equivalent of the PUREX process shown in Equation 1. The conventional PUREX process is made possible by the formation of a neutral metal-nitrato [18,19] species. Through the use of an applied electric field, ion transfer, from w→o, is achieved and, applied on an industrial scale, may elicit a new method of metal extraction. The use of ligands in FIT causes ion transfer to occur more readily and thus reduces the required amount of applied potential, the driving force. The theory of FIT has been described by the pioneering work of Homolka et al. [20], Samec et al. [21], and Girault et al. [3,4], and based on this work the stoichiometry, n, and the overall complexation constant, β, can be determined for Equation 4. However, integral to this evaluation is the degree of potential shift between the free metal formal transfer potential and the ligand assisted transfer potential. Determination of the formal transfer potential of dioxouranium is therefore necessary in order to evaluate these important thermodynamic parameters. Yet, not many formal transfer potentials of metal ions are available.

Metal ions, soluble predominantly in the aqueous phase, tend to transfer at the limit of the polarized potential window (PPW) and their $\Delta_o^w \phi^{\circ\prime}$ have been extrapolated using working curves [8,22], however, this estimate is complicated by the simultaneous transfer of supporting electrolyte ions and can generate erroneous results. It is therefore advantageous to study the transfer of these metal ions in the absence of supporting electrolyte.

In the late 1980's and early 1990's, Oldham [23,24] developed a mathematical treatment to describe the effects on the voltammetric response of little or no supporting electrolyte at a solid-liquid ultramicroelectrode (UME) interface. Oldham [24] showed that the limiting current response was three times higher in the unsupported case relative to an experiment performed using excess supporting electrolyte owing to migrational effects and the appearance of a 'linear ramp' in current; thus, the standard half-wave potential, determined using conventional data treatment techniques, would also suffer from this exaggeration, however, corrected standard potentials could be obtained if these effects were taken into account. Cyclic voltammetry (CV) and linear sweep voltammetry (LSV) conducted at ITIES hosted by microholes have

been shown to be analogous to voltammetry at recessed disc UME [9,12,25] and, thus, the adaptation of Oldham's theory towards the ITIES was performed by Wilke [25] and shown recently through curve fitting by one of our groups [12]. The mathematical treatment described by Wilke [25] was greatly simplified if the magnitude of the charge on the two components of the salt were equal; $z_i = -z_j$. However, this is not true for the current study using dioxouranium acetate dihydrate ($UO_2Ac_2 \cdot 2H_2O$) salt, where dioxouranium is 2+ and acetate is 1−. Therefore a new curve fitting approach is described herein which is applicable to any charge ratio.

The Gibbs energy of UO_2^{2+} transfer was evaluated at the aqueous|nitrobenzene (w|NB) interface [26], based on ion pair extraction of the metal ion from an acidic aqueous phase. However, this technique is complex and requires sensitive measurements of the concentration distribution between the two phases. The present method is facile and constitutes a direct, single measurement of the formal transfer potential, and thus, Gibbs energy of transfer.

We also employed finite element analysis via COMSOL Multiphysics 3.5a software to describe the kinetics of IT using Butler–Volmer formalism.

2 Simulation

Simulations were conducted utilizing finite element analysis software COMSOL 3.5a and a Butler–Volmer kinetic model described by Fick's Laws of diffusion.

Finite element analysis has proven to be effective towards describing liquid|liquid electrochemical phenomena [5,11,13,27] and especially by one of our groups with Fluxpert software for Nernstian systems [27]. Our simulation geometry, as shown in Figure 1, was designed to mimic the microhole ITIES experiments more closely by incorporating the conical shape of the microhole. As described previously [12], the microhole is generated through UV-photoablation which leaves a slightly larger radius on the side subjected to the laser beam; the microhole used in the experiment had radii of 11.2 and 13.1 μm – these dimensions were incorporated into the simulation. In general the geometry consisted of two rectangular areas termed Subdomains 1 and 2, representing the aqueous and DCE phases respectively. These two Subdomains are separated by a narrow channel which constitutes the microhole with a boundary flush to Subdomain 2 (org) hosting the ITIES. The location of the phase boundary, either on the side of the aqueous or organic phase or in between, can influence the voltammetry as has been shown [9,12,27]. Thus, its position was chosen to reflect the experimental – flush with the organic phase; in this way IT from w→o will be analogous to redox chemistry performed at a recessed microdisc electrode [9,25].

Under investigation is simple ion transfer (IT), as shown in Equation 2. The boundary conditions at the interface are described by quasireversible Butler–Volmer

(BV) formalism through Equations 5 and 6 eliciting the rate of the forward (k_f) and reverse (k_b) processes respectively:

$$k_\mathrm{f} = k° \exp\{-\alpha f(\Delta^\mathrm{w}_\mathrm{o}\phi - \Delta^\mathrm{w}_\mathrm{o}\phi°')\} \tag{5}$$

$$k_\mathrm{b} = k° \exp\{(1-\alpha)\, f\, (\Delta^\mathrm{w}_\mathrm{o}\phi - \Delta^\mathrm{w}_\mathrm{o}\phi°')\} \tag{6}$$

where $k°$ is the standard rate constant, α is the transfer coefficient, and $f = z_i F/RT$; F is Faraday's constant, R is the gas constant, and T is temperature. $\Delta^\mathrm{w}_\mathrm{o}\phi$ is the applied Galvani potential difference between the aqueous and organic phases, $\Delta^\mathrm{w}_\mathrm{o}\phi = \phi_\mathrm{w} - \phi_\mathrm{o}$, and $\Delta^\mathrm{w}_\mathrm{o}\phi°'$ is the formal transfer potential. The diffusion regime of DCE and water was considered to be approximately equivalent ($D_\mathrm{o}^i = D_\mathrm{w}^i$), this reflects that the viscosity of water and DCE are also roughly equal. Diffusion of species within the system follows Fick's laws of diffusion in axial symmetry coordinates as detailed below:

$$\frac{\partial c_\alpha^i(r,z,t)}{\partial t}$$
$$= D_\alpha^i\left(\frac{\partial^2 c_\alpha^i(r,z,t)}{\partial r^2} + \frac{1}{r}\frac{\partial c_\alpha^i(r,z,t)}{\partial r} + \frac{\partial^2 c_\alpha^i(r,z,t)}{\partial z^2}\right) \tag{7}$$
$$= D_\alpha^i \nabla c_\alpha^i(r,z,t)$$

The current generated by the transfer of ions across the ITIES was determined using the following relationship:

$$I = 2\pi z_i F \int (-D_\alpha^{\,i}\nabla c_\alpha^{\,i}(r,\,z,\,t))r\mathrm{d}r \tag{8}$$

By convention, the transfer of an ion with a positive charge from w→o generates a positive current. The potential of the LSV experiment was swept linearly forward through the use of a triangular waveform [11].

2.1 Computations

All finite element analysis was performed using an Acer Aspire laptop (Acer America Corporation (Canada), Mississauga, ON) with an Intel Core 2 Duo processor, 1.66 GHz, and 2 GB of DDR2 RAM; typical computational runtimes ranged from 3 to 5 minutes.

All curve fittings in the Oldham's regime were achieved within 40 iterations and performed using Igor Pro 6.12a (Wavemetrics Inc., Portland, OR).

3 Experimental

3.1 Chemicals

All chemicals were of reagent grade and used as purchased without further purification. Bis(triphenylphosphoranylidine)ammonium chloride (BACl) and lithium tetrakis(pentafluorophenyl) borate ethyl etherate (LiTB purum) where purchased from Acros Organics (Thermo
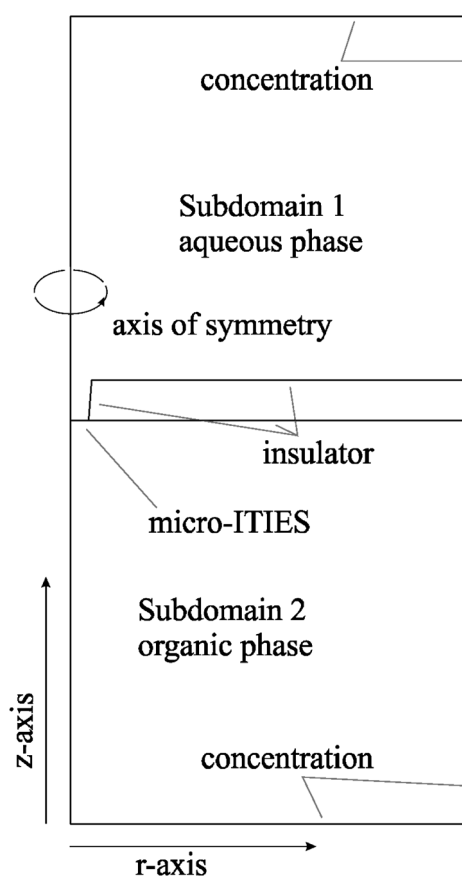
Fig. 1. Simulation geometry.

Fisher Scientific, Geel, Belgium). Lithium chloride, and tetramethylammonium bromide (TMABr) were purchased from Fluka/Sigma-Aldrich (Sigma-Aldrich Chemie GmbH, Buchs, Switzerland). BATB was prepared as has been previously described [12] through a facile metathesis reaction in a methanol:water solution (2:1, V:V); the salt was purified through recrystallization in acetone. Uranium acetate dihydrate ($UO_2Ac_2\cdot2H_2O$) was generously provided by another research group at EPFL.

3.2 Micro-ITIES

The microhole ITIES experimental apparatus consisted of two Teflon blocks with chambers fabricated into each block which housed the aqueous phase and the organic phase plus aqueous reference phase, respectively [12], as shown in Figure 2. Owing to the low current utilized in this setup, only two electrodes are necessary: one positioned in the aqueous phase and attached to the working electrode (WE) lead of the potentiostat, and the other placed in the aqueous reference phase and attached to the reference/counter (RE/CE) potentiostat leads. Both electrodes functioned as quasi-reference electrodes. The aqueous and organic phases are separated by a 25 μm thick polyamide film (Kapton, Dupont; purchased from Goodfellow, U. K.). Microholes were fabricated in the polyamide film using UV-photoablation and a metal

mask. This technique utilizes a 193 nm ArF excimer laser beam (Lambda Physik, Göttingen, Germany, fluence = 0.2 J, frequency = 50 Hz) which generates a conical hole in the film. The two diameters at either ends of the hole were determined to be 22.4 and 26.1 μm under a microscope. In this way the ratio of the diameter to the length of the channel was approximately equal, $d/L \approx 1$, as has been shown to generate reproducible results [9]. The two compartments were screwed in place with the polyamide film and a rubber o-ring in between and at the center of the two chambers; the o-ring was positioned in a circular grove fabricated into the Teflon wall which ensured a tight seal and no movement of the polyamide film. During experimental preparation the aqueous chamber was filled first with the larger diameter positioned in this phase; thus, the aqueous phase fills the microhole and the ITIES is flush with the organic phase and its behavior is analogous to a solid inlaid microelectrode [9]. The electrochemical cell examined is detailed below:

$$\text{Ag}\left|\text{AgAc}\right|\begin{matrix}0.5\,\text{mM UO}_2\text{Ac}_2\cdot 2\text{H}_2\text{O}\\(\text{aq})\end{matrix}\left\|\begin{matrix}0.5\,\text{mM BATB}\\(\text{DCE})\end{matrix}\right\|\begin{matrix}10\,\text{mM LiCl}\\5\,\text{mM BaCl}\\(\text{aq}\sim\text{ref.})\end{matrix}\left|\text{AgCl}\right|\text{Ag}\quad\text{Cell1}$$
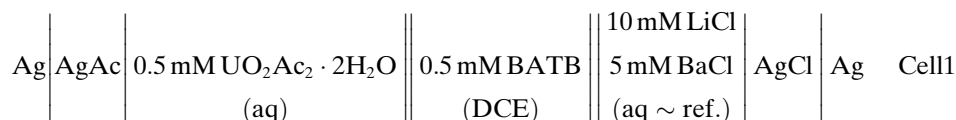
Please note that DCE was used as the organic solvent instead of the typical PUREX solvent n-dodecane [1,2], owing to its lower viscosity and since IT at the w|DCE interface is well established [3,4,7–13].
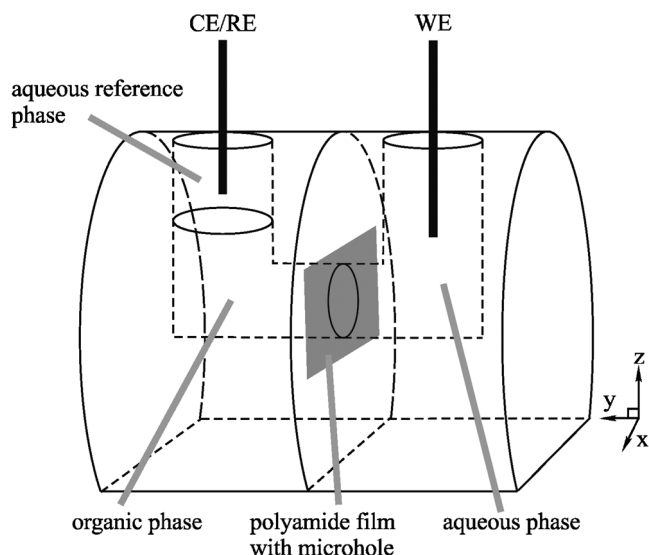
Fig. 2. Schematic of two-electrode experimental apparatus fabricated using Teflon. The w|DCE interface was supported by a microhole drilled on a 25 μm thick film of polyamide (Kapton) that was held by the two blocks tightly connected by four screws running along the *y*-axis.

3.3 Electrochemical Instrumentation

All electrochemical measurements were obtained using an Autolab potentiostat (Metrohm, Utrecht, Netherlands).

4 Results and Discussion

Figure 3 shows the experimental linear sweep voltammetry (LSV) curve (—) acquired during a scan from 0.030 to 1.550 V at a scan rate of 0.020 V·s⁻¹, after the addition of approximately 0.5 mM TMABr, in Cell 1. The steady increase in current with a half-wave potential observed at 0.160 V, and plateau at approximately 0.410 V, corresponds to the transfer of the TMA^+ cation from the aqueous to organic phase, w→o. This is quickly followed by another current increase beginning at 0.450 V which can be attributed to TB^- transfer, o→w. A final current increase is observed from approximately 0.686 to 1.200 V and is ascribed to UO_2^{2+} transfer, w→o. The transfer of TB^- and UO_2^{2+} are difficult to distinguish, however, the conclusion to separate the seemingly large sigmoidal wave from 0.450 to 1.200 V into two IT waves was brought about by three mitigating factors.

The first is based on the concentration of the analytes and the radius, *a*, of the ITIES, since the steady state current for each IT can be approximated through the following Equation for the limiting current at a planar microdisc electrode [25]:

$$I_{\text{lim}} = 4(1-z_i/z_j)\, z_i\, FD^i{}_\alpha\, c^i{}_\alpha a \tag{9}$$

The diffusion coefficient of uranium [28] has been determined for acidic solutions, as 0.4×10^{-5} cm²·s⁻¹, and is used here to determine an approximate steady state current response value; 2.16×10^{-9} A. The limiting current value determined suggests that dioxouranium itself
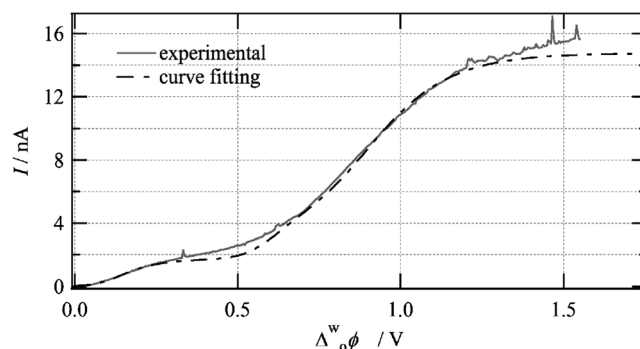
Fig. 3. LSV experimental results using Cell 1 and curve fitting obtained using Equation 13; the following experimental parameters were used: scan rate equal to 0.020 V·s⁻¹ with a potential range from 0.030 to 1.550 V.

cannot be the sole contributor and, therefore, points to the participation of another ion. The steady state current value in and of itself is not wholly significant by virtue of its approximation, however, a change in the slope of the current – potential response in Figure 3 at 0.800 V also points to a change in the ion being transferred. Finally, and most convincingly, TB^- is present in the organic phase and its formal transfer potential is well established [12], at 0.709 V, and undoubtedly transfers within the ascribed 0.450 to 1.200 V potential range. Therefore, the large sigmoidal wave was separated into two sections with the first being used to describe TB^- IT and the second for UO_2^{2+} IT.

Conventional evaluation of LSVs or cyclic voltammograms (CVs) obtained from liquid|liquid systems is to calibrate the potential scale using the TATB assumption [29,30] and known IT potentials; this technique is analogous to an internal standard method and in the present case TMA^+ IT was used as an internal reference, $\Delta_o^w\phi^{\circ\prime}=0.160$ V [31]. First the electrochemical cell is scanned, then a known concentration of internal standard is added, and the system is scanned again. In systems with an abundance of supporting electrolyte, the observed half-wave potential, $\Delta_o^w\phi_{1/2}$, is often considered equivalent to the formal transfer potential, $\Delta_o^w\phi^{\circ\prime}$, through the following relationship:

$$\Delta_o^w\phi^{\circ\prime}{}_{unknown}-\Delta_o^w\phi_{1/2,unknown}=\Delta_o^w\phi^{\circ\prime}{}_{standard}-\Delta_o^w\phi_{1/2,standard} \tag{10}$$

The addition of supporting electrolyte, however, reduces the size of the polarizable potential window (PPW) making the IT of extremely hydrophilic species unobservable [10,12]. In systems where little or no supporting electrolyte is added, it has been demonstrated [7,10,12,23–25] that the relationship $\Delta_o^w\phi_{1/2}=\Delta_o^w\phi^{\circ\prime}$ does not hold. The examination of these solutions was made accessible by the pioneering work of Oldham [23,24] who derived the theory to describe voltammetric response in unsupported systems at the solid ultramicroelectrodes (UME). Oldham's theory describes [24] the voltammetric response as one in which steady state is never actually achieved but the current continues to increase linearly with potential. This model has been adapted for use at the liquid|liquid micro-interface by the excellent work of Wilke [25] taking into account migration along with diffusion effects. In the liquid|liquid case, the continuous linear increase in current, or "linear ramp" that Oldham describes [24], is owing the migration of the counter ion in each phase away from the ITIES and towards the reference electrode or bulk solution. This migration causes a charge separation or concentration polarization within each phase between the bulk and surface concentrations at the interface [24]. Therefore, an increase in effective resistivity is induced and thus the observed "linear ramp" [24] of the current response. According to this theory [23–25] the actual half-wave potential, $\Delta_o^w\phi_{1/2,i}$, is augmented, becoming a sum of the observed half-wave potential, $\Delta_o^w\phi_{1/2,i}$, and a unit describing migration [25]:

$$\Delta_o^w\phi^{\prime}{}_{1/2j}=\Delta_o^w\phi_{1/2j}+\frac{RT}{z_jF}\ln\left[2^{-z_i/z_j}\left(1-\frac{z_i}{z_j}\right)\right] \tag{11}$$

where i and j are the anionic and cationic components of the salt under investigation.

The potential, defined as a function of the current is [25]:

$$\Delta_o^w\phi=\Delta_o^w\phi_{1/2}+\frac{RT}{z_jF}\ln\left[\left(1-\frac{z_i}{z_j}\right)\left(\frac{I}{I_{lim}-I}\right)\left(\frac{I_{lim}}{I_{lim}-I}\right)^{-z_i/z_j}\right] \tag{12}$$

If the charge ratio of the salt components is 1 ($z_i=-z_j$) than the analysis is greatly simplified and Equation 12 can be rearranged to current as a function of potential [25]:

$$I=I_{lim}\left[1+\exp\left[\frac{z_iF}{RT}\left(\Delta_o^w\phi-\Delta_o^w\phi_{1/2,i}\right)\right]\right.$$
$$\left.-\sqrt{\left[-1+\exp\left[\frac{z_iF}{RT}\left(\Delta_o^w\phi-\Delta_o^w\phi_{1/2,i}\right)\right]^2-1\right]}\right] \tag{13}$$

As has been shown recently [12], steady state IT component (the linear rise before achieving the plateau current) of the experimental curve can be fit using Equation 13, whereby z_iF/RT, $\Delta_o^w\phi_{1/2}$, and I_{lim} were determined. However, the dioxouranium acetate salt fails this criterion and thus curve fitting using Equation 13 would be erroneous. Figure 4 shows the curve fitting results (—) obtained using Equation 13 and is shown here in order to illustrate more clearly the segregation between TB^- and UO_2^{2+} IT. Additionally, since $z_i\neq-z_j$, rearranging Equation 12 in terms of current becomes a tedious mathematical procedure; therefore we chose to use Equation 12 and invert the axis of our experimental curve. In this new curve fitting method four coefficients were used: RT/z_iF, $\Delta_o^w\phi_{1/2}$, $-z_i/z_j$, and I_{lim}.

Figure 5 shows the experimental LSV (○) segmented into A, B, and C for the transfer waves of UO_2^{2+}, TB^-, and TMA^+ respectively which have been baseline corrected for each IT in order to facilitate curve fitting (results shown as, —) achieved using Equation 12. This excellent match illustrates the effectiveness of this technique for the determination of extremely hydrophilic species like dioxouranium; the highest χ^2 was observed during TB^- IT curve fitting with a result of 0.0355 – this is most likely owing to its poor resolution from the UO_2^{2+} IT. In each curve fitting the charge ratio was held constant, e.g. for UO_2^{2+} $-z_i/z_j=2$, while the I_{lim}, $\Delta_o^w\phi_{1/2}$, and RT/z_iF terms were allowed to vary; the latter term corresponds to the slope of the associated current increase
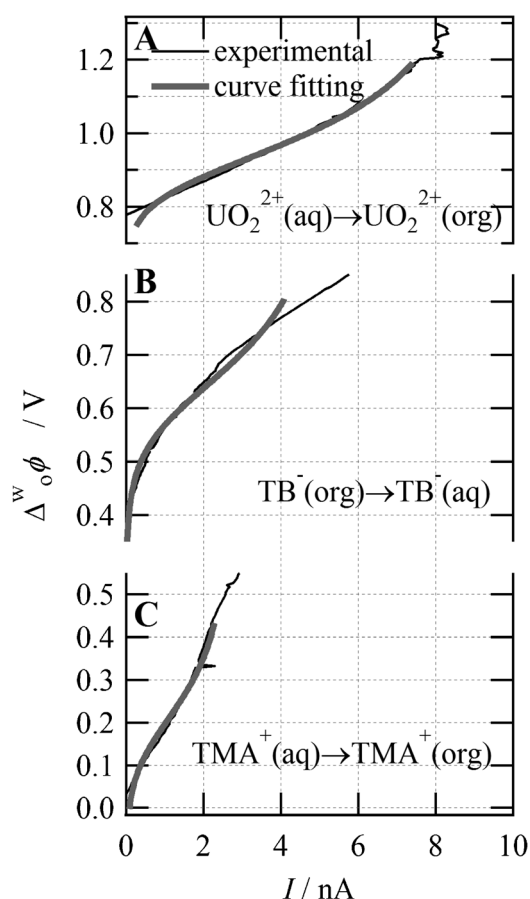
Fig. 4. Experimental (—) LSV described in Figure 3 under axis inversion and baseline corrected in A, B, and C for UO_2^{2+}, TB^-, and TMA^+ transfer respectively; each includes curve fitting (—) results obtained using Equation 12.

during IT and is calculated to be 0.0257 and 0.0128 for $z_i = 1$ and 2 respectively. After the fitting was obtained the value of RT/z_iF for UO_2^{2+}, TB^-, and TMA^+ transfer was determined to be 0.04945, 0.05453, and 0.0588 respectively. This deviation is similar to the one noted by one of our groups previous results [12] using Equation 13 with the analogous term z_iF/RT, and, as was noted in this earlier work, may be owing to a lack of separation between the ITs and the high resistivity brought about by the extreme hydrophilicity of dioxouranium. The best half-wave potential separation between the internal reference and the ion of interest to achieve optimal results has been reported to be between 0.350 and 0.450 V [12].

The formal transfer potential of UO_2^{2+}, $\Delta_o^w\phi^{o'}_{UO_2^{2+}}$, and TB^-, $\Delta_o^w\phi^{o'}_{TB^-}$, were determined to be 0.865 and 0.600 V respectively at the w|DCE interface using TMA^+ IT as the internal reference. The TB^- result is in fair agreement with recently published results, 0.709 V; [12] the difference is probably owing to its poor resolution but may also be the result of ion pair formation which has been shown to increase with increasing hydrophilicity [12]. i.e. TB's interaction/adsorption at the interface with UO_2^{2+}. The dioxouranium cation shows extreme hydrophilicity to the extent that it is one of the most hydrophilic ions yet

measured [12,22] with a $\Delta_o^w\phi^{o'}$ greater than lithium, Li^+; $\Delta_o^w\phi^{o'}_{Li^+} = 0.650$ V [12]. The transfer potential is related to the Gibbs energy of transfer via $\Delta G_{tr}^{o',w\rightarrow o} = z_iF\Delta_w^o\phi^{o'}$ such that $\Delta G_{tr,UO_2^{2+}}^{o',w\rightarrow o} = 167$ kJ mol^{-1}; compared to Li^+ which is 62.7 kJ·mol^{-1} with perchlorate as a counter ion. [12] The formal transfer potential of dioxouranium was also approximated using Equation 13 and determined to be 0.850 V; this curve fitting result (--) is illustrated in Figure 3. $\Delta_o^w\phi^{o'}_{UO_2^{2+}}$ obtained using Equation 12 and 13, are in good agreement, however, both results should be considered as estimations owing to the poor resolution of UO_2^{2+} and TB^- IT and it may be the case that these ions are, in fact, transferring simultaneously.

The Gibbs energy of transfer determined by Yoshida et al. [26] at the w|NB interface was 72 kJ·mol^{-1}, giving a formal transfer potential of 0.373 V. This value was obtained through analytical determination of several constants and the following Equation [26]:

$$\log\left(\frac{D_M^{1/z}}{D_H}\right) = \frac{\Delta G_{tr,H}^o - \Delta G_{tr,M}^o}{2.303RT} + \log\left[\frac{\gamma_{H,o}/\gamma_{H,w}}{(\gamma_{M,o}/\gamma_{M,w})^{1/z}}\right]$$
$$+ \log\left[\frac{(1 + \sum K_{i,p,MY_n,o} \times (\gamma_{M,o}/\gamma_{MY_n,w})(\gamma_{Y,o}/\gamma_{Y,o}))^{1/z}}{1 + K_{i,p,HY,o}\gamma_{H,o}c_{Y,o}}\right] \quad (14)$$

where D_i, for Equation 14 only, refers to the distribution ratio of species i and was measured using analytical techniques such as inductively coupled plasma [26]. Species Y in Equation 14 is the anionic component of the metal salt being evaluated, in that this methodology takes into account the ion pair formation of the metal with its counter ion in the organic phase as well as with H^+; the K terms in Equation 14 represent the equilibrium constants of these two reactions and were determined electrochemically by the authors [26]. The activity coefficients, $\gamma_{i,\alpha}$, of species i in phase α were calculated by an extended Debye–Hückel Equation in conjunction with an additional relationship formulated by Yoshida et al. [26] The final term to be described, $c_{Y,o}$, is the concentration of the metal species counter ion in the organic phase and was estimated by the authors via the same formulation used to evaluate the activity coefficients [26]. This approach [26] requires the use of multiple analytical techniques and draws on a deep understanding of thermodynamics. However, the Gibbs energy of transfer obtained for UO_2^{2+} is only applicable to the w|NB interface since the solvation environment, and hence transfer potential, will be particular to that solvent system [14]. Thus, while accurate, the $\Delta_{NB}^w\phi^{o'}_{UO_2^{2+}}$ determined by Yoshida et al. [26] cannot be used at the w|DCE ITIES and, therefore, what is presented herein is a facile, unidisciplinary approach for the determination of the formal transfer potential of dioxouranium. It should be noted that the transfer potential UO_2^{2+} at the w|NB [26] interface is much lower than that determined here at DCE. While this translates to less applied potential required to elicit uranyl transfer it also means that the w|NB ITIES will have a narrower
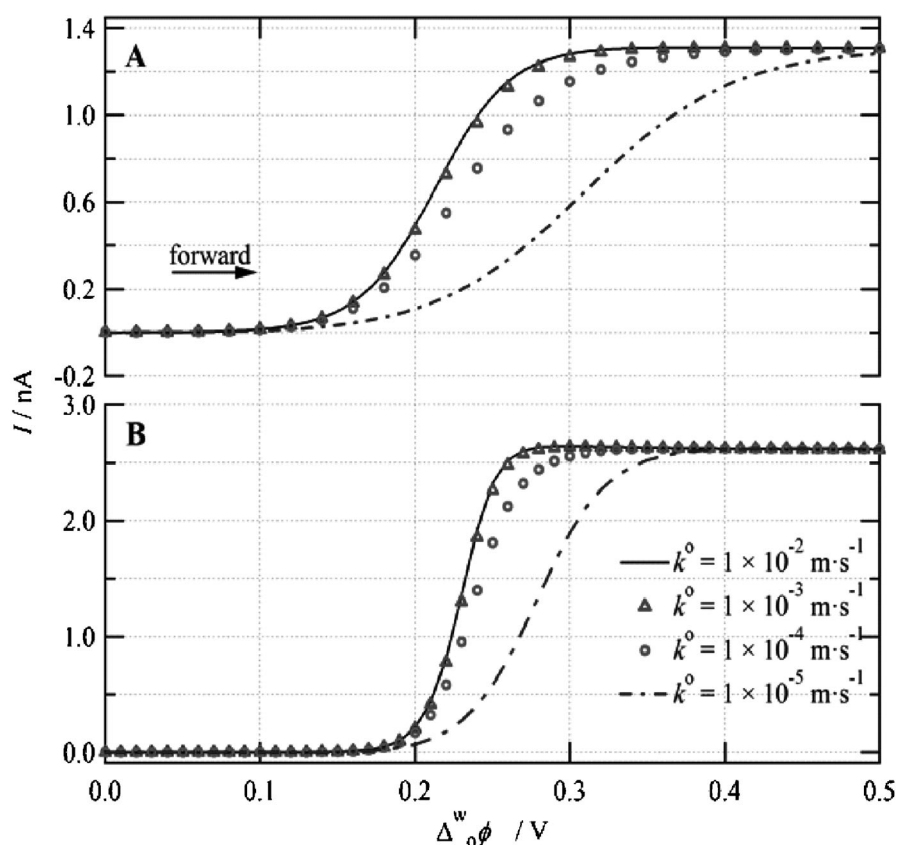
Fig. 5. Simulated LSVs obtained using the microhole geometry depicted in Figure 1, with $z_i = 1$ and 2 for A and B respectively. The following parameters were used in both: $\alpha = 0.5$, $c_w^i = 1.0$ mM, $c_o^i = 0.0$ mM, $v = 0.020$ V·s^{-1}, $\Delta_o^w \phi_i^{0\prime} = 0.250$ V, and varying k° as indicated in the legend.

PPW than that experienced at a w | DCE interface. A narrower PPW also means that less IT and FIT can be observed and quantified; hence this is why DCE is a valuable organic solvent for studying FIT.

In order to garner more insight into the kinetics of IT at a microhole interface, this system was studied using finite element analysis with the geometry shown in Figure 1. The boundary condition at the interface was set to follow Butler–Volmer (BV) formalism. And the UO_2^{2+} diffusion in the two domains obey Fick's laws of diffusion.

Figures 5A and B show simulation LSV curves obtained using $z_i = 1$ and 2 respectively and $\alpha = 0.5$, $c_w^i = 1.0$ mM, $c_o^i = 0.0$ mM, $v = 0.020$ V·s^{-1}, $\Delta_o^w \phi^{0\prime} = 0.250$ V, and with k° values of 1, 0.1, 0.01, and 0.001 cm·s^{-1}. The diffusion coefficients for both phases were held at 1×10^{-5} cm^2·s^{-1}. When $k^\circ = 1.0$ cm·s^{-1} the curves shown in Figure 5A and B are in good agreement with those calculated by Wilke [25] and obtained by Josserand et al. [27] using a Nernstian model. By augmenting the standard rate constant the overall kinetics of the reaction can be changed which alters the slope of linear approach to the steady state current. As shown in Figure 5, with smaller values of k_o the slope of the linear portion of the curve, before the current plateaus, decreases and the half-wave potential shifts; this resembles the change predicted by Oldham's theory of redox chemistry performed in the ab-

sence of supporting electrolyte [23,24]. Figure 5B indicates that, with increased charge, slower reaction kinetics have a reduced effect on the slope of the IT curve. Therefore, migration effects associated with IT in systems with little or no supporting electrolyte was approximated using slow BV kinetics.

Each IT was examined individually and compared versus the LSVs obtained experimentally with an initial concentration of 0.5 mM where UO_2^{2+} and TMA$^+$ were present only in the aqueous phase (Subdomain 1 in Figure 1) and TB$^-$ only in the organic phase. The diffusion coefficient, standard rate constant, and transfer coefficient were varied until a good overlap was achieved; the final standard rate constant, k°, and transfer coefficient for each ion was maintained at 1×10^{-3} cm·s^{-1} and 0.5 while the diffusion coefficients, $D_w^i = D_o^i$, for, TB$^-$, and TMA$^+$ were equal to 2.6, and 1.4×10^{-5} cm^2·s^{-1} respectively. Two diffusion coefficients for UO_2^{2+} were used: 1.0 and 7.5×10^{-5} cm^2·s^{-1} as shown in Figure 6B as ($\triangle$) and ($\circ$) curves respectively. The first value was obtained by using the limiting current value generated during curve fitting via Equation 12; this value was then used to solve for D in Equation 9 and is in fair agreement with that demonstrated previously [28]. The latter UO_2^{2+} diffusion coefficient was determined through iterative simulations to best approximate the steady state current obtained experimentally. The formal transfer potentials used

in the simulation were also varied, for TMA$^+$, TB$^-$, and UO$_2^{2+}$ IT the final values were 0.143, 0.490, and 0.983 V respectively and these are in fair agreement with those obtained from the curve fitting results.

Figure 6B, C, and D contain the individual overlaid simulation curves (○) obtained for the respective IT of UO$_2^{2+}$, TB$^-$, and TMA$^+$ with the experimental data under baseline correction. Figure 6C and D demonstrate the effective overlap of the simulation results to the experimental and indicates that IT in the absence of supporting electrolyte can be successfully approximated using a BV model; augmenting only the diffusion coefficient and the standard rate constant can achieve a reasonable approximation of migration effects. Figure 6A includes a simulation curve whereby both TMA$^+$ and TB$^-$

ions are considered simultaneously and overlaid on the experimental results generating a good overlap.

However, Figure 6B, showing the curve obtained for UO$_2^{2+}$ IT, which constitutes the edge of the PPW, is poor. This situation remained despite utilizing a range of different $k°$ values from 1×10^{-3} to 1×10^{-10} cm·s^{-1} for both diffusion coefficients and is most likely owing to the high ohmic polarization induced at the ITIES combined with total ion depletion near the interface. The experimental curve and the simulation curve, obtained with $D_{UC_2^{2+}}$ equal to 1.0×10^{-5} cm^2·s^{-1}, in Figure 6B are similar to Figure 10 shown in Oldham's previous work [24] where he describes an analogous redox scenario as follows:

$$R^{2-} \rightarrow 2e^- + P \tag{15}$$
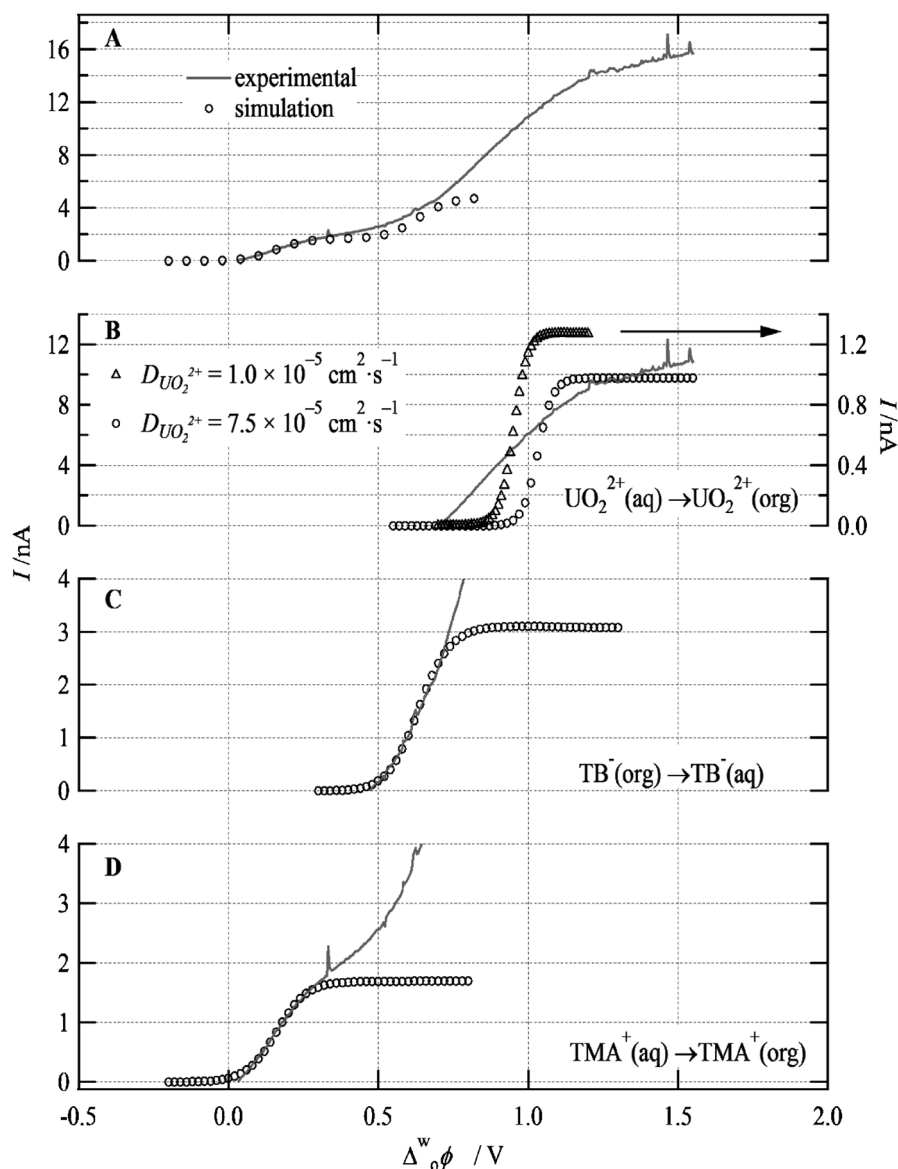
Fig. 6. (A) contains the experimental results as described in Figure 3 with an overlay of the TMA$^+$ and TB$^-$ simulated IT. (B), (C), and (D) illustrate the individual, baseline corrected experimental LSVs overlaid with the simulated IT for UO$_2^{2+}$ (w→o), TB$^-$ (o→w) and TMA$^+$ (w→o), respectively. The simulation parameters were as follows: $\alpha = 0.5$, $k° = 1 \times 10^{-3}$ cm·s^{-1}, $c_a^i = 0.5$ mM, with $D_w^i = D_o^i = 7.5$, 2.6, and 1.4×10^{-5} cm^2·s^{-1} and $\Delta_o^w \phi°' = 1.400$, 0.941, and 0.593 V for UO$_2^{2+}$, TB$^-$, and TMA$^+$ respectively.

In this scenario the electroactive species, R^{2-}, is oxidized to the product, P, liberating two electrons; not shown is the counter ion, C, which has a charge of 1+ [24]. As the reaction shown in Equation 15 proceeds, the concentration profiles of R^{2-} and C^+ decrease at similar rates with distance from the electrode surface [24]; this results in a large ohmic polarization. Oldham [24] compared the theoretical LSVs and showed that, in the above example, the curve without supporting electrolyte has a steady state current three times higher than that with supporting electrolyte. Within the present simulation parameters only two terms exist which can increase the steady state current: the initial concentration of the ion being transferred and the diffusion coefficient. Therefore an effective diffusion coefficient was used to approximate the ohmic polarization and thus this value is much higher than the uranyl diffusion coefficient given in the literature [28]. While this does demonstrate excellent agreement with the experimental steady state value, it does not overlap well with the linear rise in the current response. Additionally, curve ($\triangle$) in Figure 6B shows the simulation response using a smaller diffusion coefficient and is what would be expected should the system have adequate supporting electrolyte.

Therefore, the BV model can be used to describe most IT. But in extreme cases, as with UO_2^{2+} IT, where the ion demonstrates extreme hydrophilicity, the simulation result indicates there is a limitation to the BV kinetic model and a more complex strategy must be broached.

A mixed diffusive and migrational model considers the current density at the interface as a linear combination of the diffusion, i_d, and migration, i_m, components such that [32]:

$$i = i_d + i_m \tag{16}$$

And the flux of charged species, in a solution without convection, can be described by the Nernst–Planck Equation [32]:

$$J_i(x) = -D_\alpha^i \nabla c_\alpha^i - \frac{z_i F}{RT} D_\alpha^i c_\alpha^i \nabla \phi \tag{17}$$

TMA^+ and TB^- ions transfer at relatively low applied potential compared to dioxouranium, and, since the migration effect is proportional to the magnitude of the applied electric field [23,25,32], it follows that the migrational component of the flux of these ions across the interface is minimal. Thus TMA^+ and TB^- IT can be easily predicted by BV kinetics and Fick's Laws of diffusion, while UO_2^{2+} cannot since the applied potential (hence migration) is much greater. We are presently working towards a more complex simulation which will include BV IT kinetics in conjunction with a Nernst–Planck description of ion movements in either phase so as to better approximate IT in unsupported electrochemical solutions as described by Oldham [23,24] and Wilke [25]. The BV model, with ion movement governed only by Fick's Laws

of diffusion, is a facile approach which provides a good approximation for most of the ions in solution, however, in extreme cases a more complex model may be necessary.

5 Conclusions

Herein was described the IT of UO_2^{2+} across a w|DCE ITIES supported by a 25 μm diameter microhole, without supporting electrolyte. Using the theory developed by Oldham [23–24] and Wilke [25] the formal transfer potential, $\Delta_o^w \phi_{UO_2^{2+}}^{o'}$, for dioxouranium has been determined to be 0.865 V.

Ion transfer was studied, with COMSOL Multiphysics 3.5a, to describe the kinetics of IT using a BV model. The LSV obtained utilized the following parameters: $\alpha = 0.5$, $k^\circ = 1 \times 10^{-3}$ cm·s^{-1}, and D_α^i for UO_2^{2+}, TB^-, and TMA^+ equal 7.5, 2.6, and 1.4×10^{-5} cm^2·s^{-1} respectively to obtain good overlap with the simulation versus the experimental results for all but dioxouranium. Since this BV model considered only the diffusive component, the simulation might be improved by augmenting the flux of the electroactive species through the utilization of the Nernst-Planck Equation. Aoki did some pioneering work on ion transfer kinetics at a viscous interface using the Langenvin Equation [33].

Supporting Information

The curve fitting procedure, written in Igor (Igor Pro 6.12a), and the report for COMSOL (COMSOL 3.5a) code used to simulate the linear scan voltammogram, using Butler–Volmer formalism. The simulation code and curve fitting program are available from the authors upon request.

References

[1] A. P. Paiva, P. Malik, *J. Radioanal. Nucl. Chem.* **2004**, *261*, 485.

[2] K. L. Nash, in *Separations for the Nuclear Fuel Cycle in the 21st Century* (Eds: G. J. Lumetta, K. L. Nash, S. B. Clark, J. I. Friese), ACS, Washington, DC **2006**, pp. 22–40.

[3] F. Reymond, P.-A. Carrupt, H. H. Girault, *J. Electroanal. Chem.* **1998**, *449*, 49.

[4] F. Reymond, G. Lagger, P.-A. Carrupt, H. H. Girault, *J. Electroanal. Chem.* **1998**, *451*, 59.

[5] N. Nishi, H. Murakami, S. Imakura, T. Kakiuchi, *Anal. Chem.* **2006**, *78*, 5805.

[6] J. Langmaier, A. Trojanek, Z. Samec, *Electroanalysis* **2009**, *21*, 1977.

[7] M. C. Osborne, Y. Shao, C. M. Pereira, H. H. Girault, *J. Electroanal. Chem.* **1994**, *364*, 155.

[8] G. Lagger, L. Tomaszewski, M. D. Osborne, B. J. Seddon, H. H. Girault, *J. Electroanal. Chem.* **1998**, *451*, 29.

[9] S. Peulon, V. Guillou, M. L'Her, *J. Electroanal. Chem.* **2001**, *514*, 94.

[10] F. Li, Y. Chen, M. Q. Zhang, P. Jing, Z. Gao, Y. H. Shao, *J. Electroanal. Chem.* **2005**, *579*, 89.

[11] P. J. Rodgers, S. Amemiya, *Anal. Chem.* **2007**, *79*, 9276.

[12] A. J. Olaya, M. A. Méndez, F. Cortes-Salazar, H. H. Girault, *J. Electroanal. Chem.* **2010**, *644*, 60.

[13] T. J. Stockmann, Z. Ding, *J. Electroanal. Chem.* **2010**, *649*, 23.

[14] Z. Samec, J. Langmaier, T. Kakiuchi, *Pure Appl. Chem.* **2009**, *81*, 1473.

[15] H. Girault, in *Electroanalytical Chemistry*, Vol. 23 (Eds: A. J. Bard, C. G. Zoski), CRC Press, Boca Raton, FL **2010**, pp. 1–104.

[16] H. H. J. Girault, D. J. Schiffrin, in *Electroanalytical Chemistry*, Vol. 15 (Ed: A. J. Bard), Marcel Dekker, New York **1989**, pp. 1–141.

[17] R. A. W. Dryfe, in *Adv. Chem. Phys.*, Vol. 141 (Ed: S. A. Rice), Wiley, New York **2009**, pp. 153–215.

[18] J. H. Burns, *Inorg. Chem.* **1981**, *20*, 3868.

[19] J. H. Burns, *Inorg. Chem.* **1983**, *22*, 1174.

[20] D. Homolka, K. Holub, V. Marecek, *J. Electroanal. Chem. Interf. Electrochem.* **1982**, *138*, 29.

[21] Z. Samec, D. Homolka, V. Marecek, *J. Electroanal. Chem. Interf. Electrochem.* **1982**, *135*, 265.

[22] Y. Shao, A. A. Stewart, H. H. Girault, *J. Chem. Soc. Faraday Trans.* **1991**, *87*, 2593.

[23] K. B. Oldham, *J. Electroanal. Chem.* **1988**, *250*, 1.

[24] K. B. Oldham, *J. Electroanal. Chem.* **1992**, *337*, 91.

[25] S. Wilke, *J. Electroanal. Chem.* **2001**, *504*, 184.

[26] Y. Yoshida, Z. Yoshida, H. Aoyagi, Y. Kitatsuji, A. Uehara, S. Kihara, *Anal. Chim. Acta* **2002**, *452*, 149.

[27] J. Josserand, J. Morandini, H. J. Lee, R. Ferrigno, H. H. Girault, *J. Electroanal. Chem.* **1999**, *468*, 42.

[28] Y. Awakura, K. Sato, H. Majima, S. Hirono, *Metall. Trans. B* **1987**, *18*B, 19.

[29] B. G. Cox, A. J. Parker, *J. Am. Chem. Soc.* **1973**, *95*, 6879.

[30] A. J. Parker, *Electrochim. Acta* **1976**, *21*, 671.

[31] T. Wandlowski, V. Marecek, Z. Samec, *Electrochim. Acta* **1990**, *35*, 1173.

[32] A. J. Bard, L. R. Faulkner, *Electrochemical Methods: Fundamentals and Applications*, 2nd ed., Wiley, New York **2001**.

[33] K. Aoki, *Electrochim. Acta* **1996**, *41*, 2321.